



## CHLORIDE-ION INDUCED CORROSION OF GALVANIZED AND ORDINARY STEEL REINFORCEMENT IN HIGH-PERFORMANCE CONCRETE

N. Gowripalan<sup>1</sup> and H.M. Mohamed

School of Civil and Environmental Engineering, University of New South Wales,  
Sydney 2052, Australia

(Received February 6, 1998; in final form June 2, 1998)

### ABSTRACT

An experimental investigation has been carried out to assess the effectiveness of the use of high-performance concrete (HPC) and galvanized steel in reducing reinforcement corrosion. Two normal strength concrete (NSC) mixtures with 28-day compressive strengths of 30 and 40 MPa and two high strength concrete (HSC) mixtures with compressive strengths of 50 and 80 MPa were used for this study. The rapid chloride ion penetration test was used to study the ion penetration and the results are compared with the results of long-term immersion tests in 4% NaCl solution over a period of 1 year. No correlation between the results of these two tests could be established. Half-cell potential measurements were used to monitor the initiation of corrosion. The pH of HPC pastes and mortars were monitored for 90 days to study the effect of silica fume on pH of concrete and corrosion initiation. The results showed that HPC reduced chloride ion penetration significantly. Silica fume at 10% replacement level reduced the pH of concrete from 14.00 to 12.8 over a period of 90 days. © 1998 Elsevier Science Ltd

### Introduction

The corrosion of steel reinforcement in concrete is caused by carbonation of concrete or by the presence of chloride ions or similar aggressive species. Chloride-induced corrosion of reinforcement is one of the major causes of deterioration leading to a reduced service life of reinforced concrete structures. In the presence of chloride ions, the breakdown of the passive oxide layer, even at high pH levels, at the concrete-steel interface is the most common cause that initiates pitting corrosion of steel reinforcement. The subsequent rate of corrosion depends on the availability of oxygen and water near the interface, and is thus a function of the permeability of the concrete protecting the steel. In addition, the environmental regime plays a major role, with alternate wetting and drying being one of the most severe conditions.

One of the measures that can be taken to improve the durability of a concrete structure is to increase the resistance of concrete to permeation of chloride ions. High-performance concrete (HPC) containing silica fume, slag, or fly ash is characterized by its improved pore

<sup>1</sup>To whom correspondence should be addressed.

structure with a dense matrix and low permeability, and these factors can offer protection against corrosion. Other means of protection will include cathodic protection or coating reinforcement with epoxy (epoxy coated bars) or zinc (galvanized steel).

Hot-dip galvanizing is one of the most important zinc-coating processes used to produce galvanized steel bars. In this process, a hot zinc bath is maintained at about 450–460°C. At this temperature, the reaction between zinc and iron or steel is at first rapid and then usually slows down, the rate of coating being related to the type of steel. The reaction produces several specific zinc/iron compounds, which form layers in the coating. A layer of pure zinc solidifies on the outside of the bar (1).

Fundamentally, steel corrosion is an electrochemical process, and a metal coating such as zinc can protect the steel. In the presence of an electrolyte, a current will flow from the steel to the zinc; zinc becomes an anode and the steel a cathode. Zinc corrodes in preference to steel, and in doing so protects the steel surface. Chloride ions have far less effect on the corrosion of zinc than on the corrosion of steel except in flowing sea water and brackish water (1).

Blended cements have received considerable attention in recent years due to their significantly superior durability performance in aggressive exposure conditions. Silica fume is one of the mineral admixtures which reduces concrete permeability significantly. The beneficial effect of supplementary cementitious materials, such as silica fume, has been attributed to the refined, less continuous pore structure which leads to a decrease in permeability and chloride ion penetration (2). The slight reduction in the pH of concrete by the addition of silica fume, which may cause depassivation of the protective oxide layer of steel, is sometimes regarded as a problem. However, at typical replacement levels, even up to 20% by mass of cement, the reduction in pH is not large enough to cause any concern.

## Scope

In this investigation, two mixtures with normal Portland cement and another two with a Portland cement/silica fume blend were tested. The w/b varied from 0.25 to 0.55. The expected characteristic strength at 28 days varied from 30 to 80 MPa. Specimens tested varied in size from 50 mm diameter cylinders to 100 mm diameter cylinders and  $150 \times 150 \times 150$  mm cubes with embedded bars having different concrete cover. The cover varied from 10 mm to 50 mm in thickness. Only simple techniques such as immersion in salt solution, wetting and drying cycle of salt solution, rapid chloride ion penetration test, and half-cell potential were used to characterize the concrete permeability and corrosion rate of steel. The wetting and drying cycles consisted of 24 h salt water spraying followed by 24 h drying at about 35°C.

## Materials Used

### Cement

The cement used was of Type GP (Type A), similar to ASTM Type I. The oxide composition of the cement used is given in Table 1.

TABLE 1  
Chemical analysis of cement and silica fume used.

Oxide composition	Type GP (Type A) cement (%)	Silica fume (%)
SiO <sub>2</sub>	22.0	94
Al <sub>2</sub> O <sub>3</sub>	4.5	0.4
Fe <sub>2</sub> O <sub>3</sub>	3	0.7
CaO	62	0.3
MgO	3	0.1
SO <sub>3</sub>	3	0.15
Na <sub>2</sub> O	0.5	0.2
K <sub>2</sub> O	0.8	0.3
Loss on ignition	1.5	3.0

### Silica Fume

The silica fume used was an Australian silica fume with the composition and characteristics given in Tables 1 and 2.

### Aggregates

For all mixes, 10 mm crushed basalt and Sydney sand were used as coarse and fine aggregates, respectively.

### Superplasticizer

A combination of sulphonated naphthalene-formaldehyde and melamine-formaldehyde condensates that is readily available in Australia was used as the superplasticizer.

TABLE 2  
Physical properties of cement and silica  
fume used.

Physical properties	Type GP (Type A) cement	Silica fume
Specific gravity	3.15	2.20
Fineness (surface area) Sq.m/kg	400	19,000
Compressive strength at 28 days (MPa)	37.0	—

**TABLE 3**  
Details of mixture proportions of the four test series.

Materials	Mixture proportions (kg/m <sup>3</sup> )			
	I (NSC)	II (NSC)	III (HSC)	IV (HSC)
Cement	350	350	500	500
Silica fume	0	0	55	55
Water	193	158	190	140
Water/binder	0.55	0.45	0.35	0.25
Fine aggregate	616	616	685	640
Coarse aggregate	1,251	1,251	1,000	1,170
Superplasticizer (L)	0	1.75	5.67	11.67
Expected comp. str. at 28 days (MPa)	30	40	50	80
Actual comp. str. at 28 days (MPa)	29.1	34.6	50.1	82.1

### Mixture Proportions

Four series of concrete mixtures were prepared for this study. Series I and II were normal strength concrete (NSC) mixtures and the w/b (or w/c for these two mixtures) was 0.55 and 0.45, respectively. Series III and IV were high-strength concrete mixtures, both having 10% of normal Portland cement replaced by silica fume (by mass of cement) and a w/b of 0.35 and 0.25, respectively. The basic mixture proportions of the concrete were chosen to obtain slumps of 50–70mm and 28-day characteristic strengths of 30, 40, 50, and 80 MPa. The details of mixture proportions and cylinder compressive strengths at 28 days for all four series are shown in Table 3.

### Preparation of Specimens

The materials were mixed in a pan mixer in the laboratory and the specimens were cast in steel molds, except for the 50 mm diameter specimens. The latter specimens were cast in disposable cardboard molds. 2 h after casting, the specimens were covered with wet hessian and polythene sheets and were kept in a controlled temperature-humidity room (at 23°C and 50% relative humidity) for 24 h prior to demolding. After demolding, the specimens were cured in a fog room (23°C and 95% relative humidity) until testing.

Uncoated deformed steel and galvanized deformed steel bars of 12 mm diameter were embedded concentrically in cylindrical specimens made from all four mixtures. The cylinders having covers of 20 and 40 mm were subjected to wetting and drying cycles starting at the age of 28 days. In addition, 150 × 150 × 150 mm cubes with embedded bars with different cover were also prepared for testing. The top face of all specimens was sealed with an epoxy (15–20 mm thick) to prevent any chloride ion ingress through this surface.

## Testing of Specimens

### Rapid Chloride Ion Penetration Test (RCPT)

The RCPT was performed according to ASTM C1202-91 (3). Sodium hydroxide (0.3 N) and 3% sodium chloride were placed in the chambers on either side of a concrete specimen (100 mm diameter and 50 mm thick), and a direct current voltage of 60 V was applied across the two faces. The current passing through the concrete specimen was monitored at regular intervals over a period of 6 h, and the total charge in Coulombs (current in Amperes multiplied by time in seconds) was computed.

### Corrosion Monitoring by Half-Cell Potential

The half-cell potential of the reinforcement was monitored every week using a Cu/CuSO<sub>4</sub> reference electrode (4).

### pH Test

A mass of 100 g of normal Portland cement was mixed with 200 g of distilled water. The pH of the resulting paste was monitored by a digital pH meter every 30 min. up to 7 h. The same amounts of silica fume and water were mixed separately, and the pH of this mixture was monitored at the same time intervals. The pH of a mixture with 10% silica fume replacement (a mixture of 90 g normal portland cement, 10 g silica fume, and 200 g of distilled water) was also measured for 7 h at 30-min. intervals.

For long-term pH measurement, cement pastes and mortars having same w/b as in the concrete mixtures were cast. The hardened paste or mortar samples were crushed and saturated with distilled water before measuring the pH. The pH was measured at 1, 3, 7, 14, 21, 28, 56, and 90 days of age.

## Test Results and Discussion

### Galvanized Coating

The cross sections of a typical galvanized bar that was photographed by a scanning electron microscope (SEM) are illustrated in Figure 1a (uniform coating thickness) and Figure 1b (non-uniform thickness). Figure 1a shows approximately 100  $\mu\text{m}$  thick, uniform zinc coating with the three regions clearly identified: the steel surface, the zinc/steel compounds (about 20–40  $\mu\text{m}$  in thickness), and pure zinc on the surface. Figure 1b shows non-uniformities in the coating thickness, which occur particularly when coating deformed steel bars. Figures 2a and b show the surfaces of corroded galvanized steel bars in normal-strength and high-strength concrete mixtures after 1 year of exposure in a wet and dry environment.

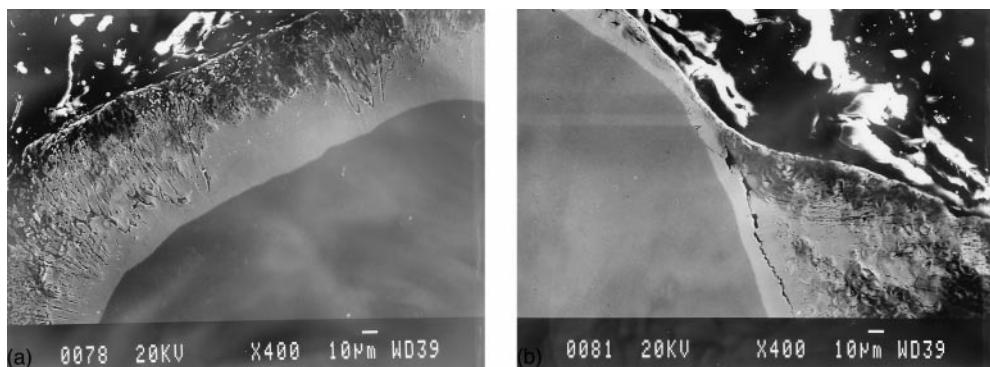


FIG. 1.

*a)* Zinc coating of galvanized steel. *b)* Non-uniform thickness of zinc coating.

### Compressive Strength Development

Cylinder compressive strength development of the different mixtures is illustrated in Figure 3. This indicates that low w/b and the presence of silica fume contribute significantly to early strength development, due to rapid and dense growth of the strong calcium silicate hydrate (C-S-H) particles (silica fume acts as nucleus) and reduced porosity. Silica fume also reacts with the weak  $\text{Ca}(\text{OH})_2$  and forms strong C-S-H particles, thereby reducing the porosity at the paste-aggregate interface.

### Rapid Chloride Ion Penetration Test (RCPT)

The relationship between the charge passed in Coulombs and the time elapsed during testing for the four series of mixtures is shown in Figures 4–6. The total charge passed in 6 h through the various concrete mixtures at 7, 28, 56, and 90 days of age is shown in Figure 7. At the age of 7 days, the charge passed in 6 h through the four mixtures varies uniformly with the w/b as shown in Figure 4. At 28 and 90 days of age, however, the distinction between the

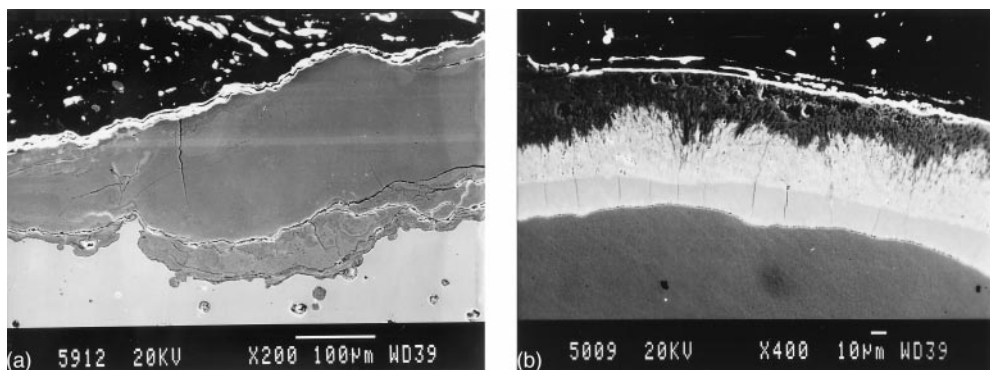


FIG. 2.

*a)* Severe corrosion of galvanized steel embedded in normal-strength concrete. *b)* Mild corrosion of galvanized steel embedded in high-strength concrete.

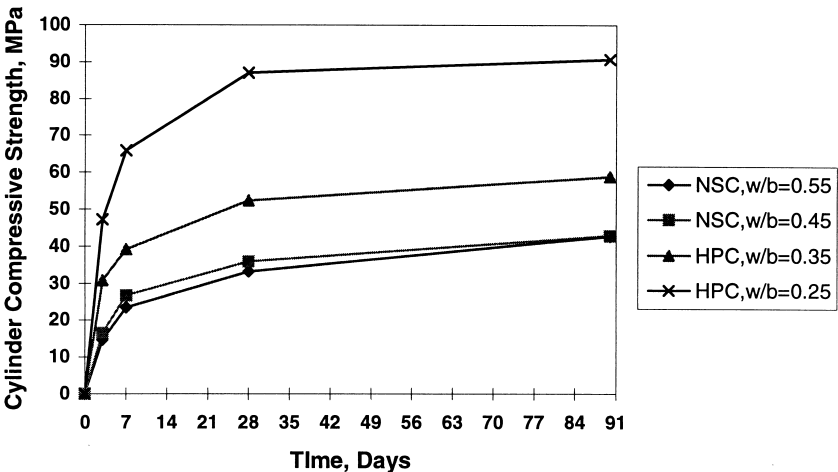


FIG. 3.  
Compressive strength development of the four concrete mixtures.

lower w/b mixtures and higher w/b mixtures (NSC mixtures) becomes clear. At 28 days of age, normal concrete mixtures with w/b 0.55 and 0.45 have values in excess of 4,000 Coulombs, while the mixtures with w/b of 0.25 and 0.35 have low values, below 900 Coulombs. This improvement is due to a combination of low w/b, and the presence of silica fume in the binder. The two low w/b mixtures (Series III and IV), with 7-day compressive strengths of 35.7 and 66.2 MPa, exhibit total charge values of 3,700 and 1,939 Coulombs, respectively. The two NSC mixtures (Series I and II) at the same age show total charge values

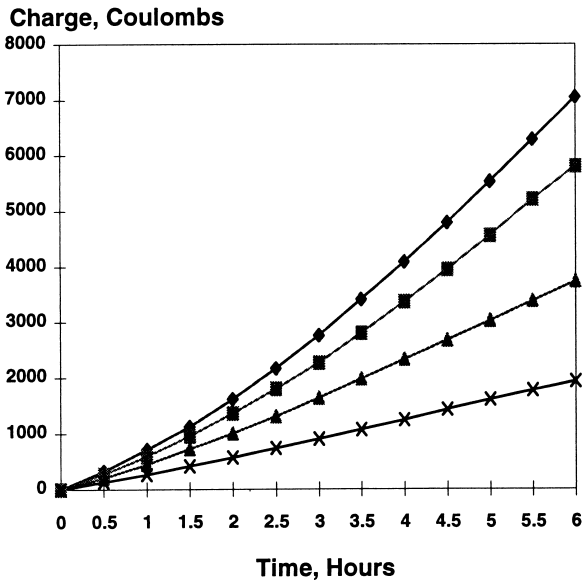


FIG. 4.  
Total charge passed through different concrete mixtures at 7 days' age.

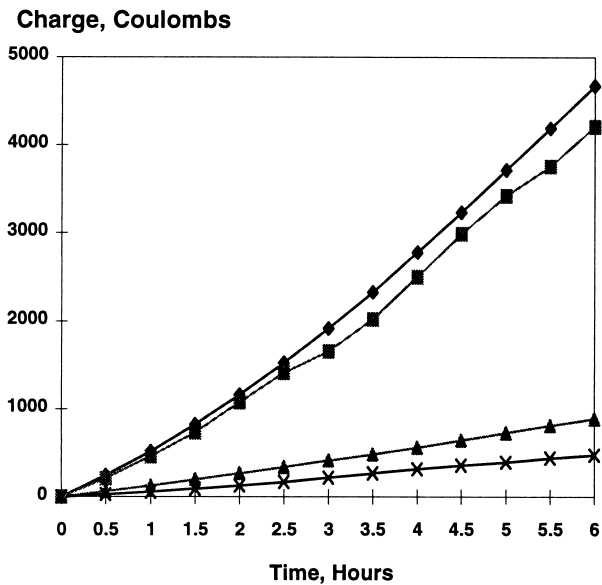


FIG. 5.

Total charge passed through different concrete mixtures at 28 days' age.

of 7,000 and 5,800 Coulombs, while the compressive strengths are 23.2 and 28.2 MPa, respectively. At 28 days of age, the total charge passed through Series III and IV reduce significantly to values of 889 and 477 Coulombs, while the values for the NSC mixtures do not improve much with continued curing.

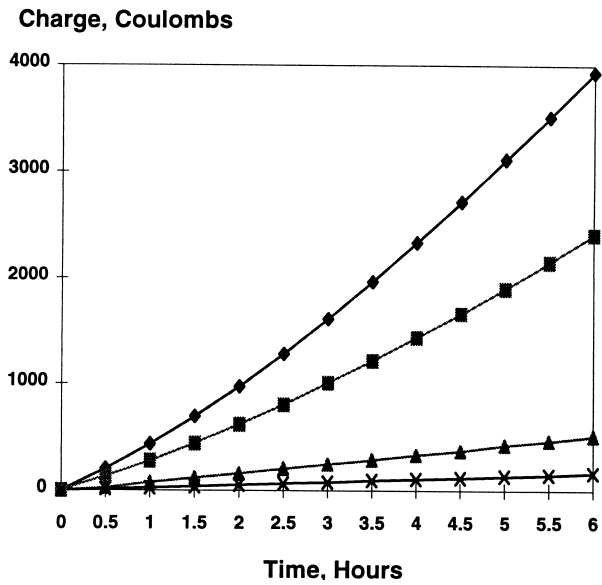


FIG. 6.

Total charge passed through different mixtures at 90 days' age.



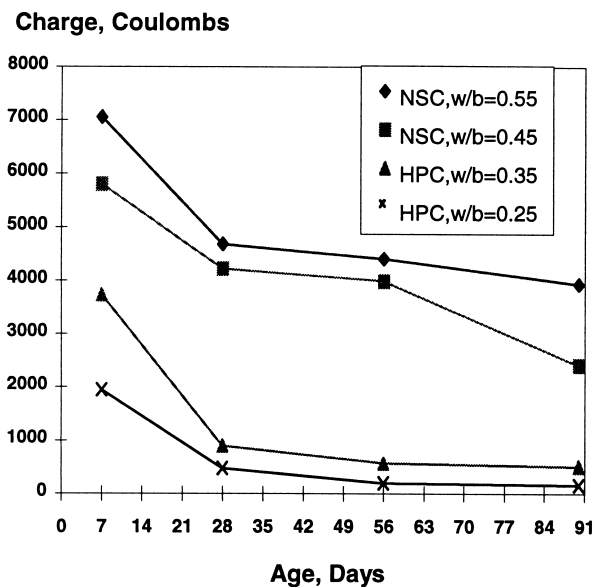


FIG. 7.

Total charge passed (in 6 h) through concrete, as a function of age.

The RCPT, as a test method, has received several criticisms as discussed by Andrade (5). The obvious uncertainty indicated by Andrade is that the total charge measured is based on the total current and not on the component corresponding to the chloride ion flow, because part of the current would be due to the movement of other ions through the concrete. Also, during testing of high-permeability concrete mixtures, a considerable amount of heat is produced, which in turn changes the flow characteristics of the ions. For some mixtures, with an applied voltage of 60V the authors observed a 33°C temperature rise during the 6 h period of the test (6). This test is fundamentally a resistance test and not a permeability test. Hence, the results will be affected by the conductivity of the pore solution as well as the nature of the porosity.

Despite these uncertainties, this is one of the most popular tests for comparing the performance of concrete with admixtures, repair materials, and coating systems (7–10). This test, or a modified version, has also been incorporated in other national standards (11). It is a convenient test and can be conducted in a much shorter time than other permeability tests. These are some of the reasons why the RCPT has been widely used as a comparative test method. Ozyildirim (7,10) has studied a large number of samples containing different mixture compositions of concrete, and by a ponding test has found that there is a qualitative relationship between the Coulomb values and the chloride ion penetration. More work in this area with modified RCPT methods (e.g., lower voltages, longer monitoring time, isothermal flow conditions, steady state and non-steady state flow conditions) is currently in progress in order to establish whether a modified RCPT can be correlated to long-term chloride ion migration tests.

## pH Results

The relationship of initial pH and time (in hours) for pastes (w/b of 2.0) is illustrated in Figure 8. The pH of normal Portland cement ranges from 12.39–12.63, while the pH of pure silica

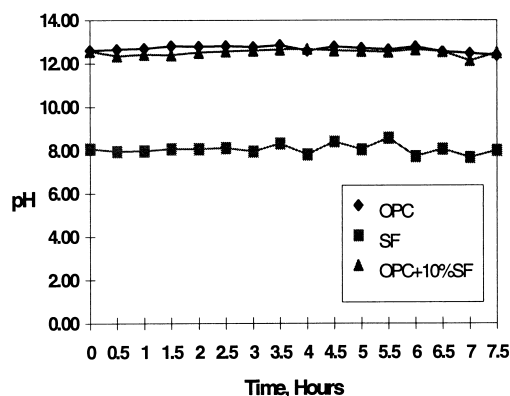


FIG. 8.

Initial pH of different cement pastes.

fume has a range between 7.49–8.50. With lower w/b, as used in Portland cement concrete mixtures, a higher pH can be expected. The replacement of cement by silica fume at the 10% level has a negligible influence on the initial pH of the paste.

After 24 h, the pure cement and blended cement pastes became hardened and the measurement of pH by the embedded probe was not possible. Therefore, cement pastes and mortars with identical w/b as in the concrete mixtures were cast and the pH was monitored as described earlier. The results of pH of hardened cement pastes are shown in Figure 9. The pH values of the cement pastes of HSC are very high, almost reaching 14.00 at the early ages. However, within the first 7 days there is a substantial reduction in pH. After this age, the change in pH is gradual, as in NSC mixtures. For NSC mixtures with w/b 0.55 and 0.45, the change in pH is gradual over the entire period of 90 days with

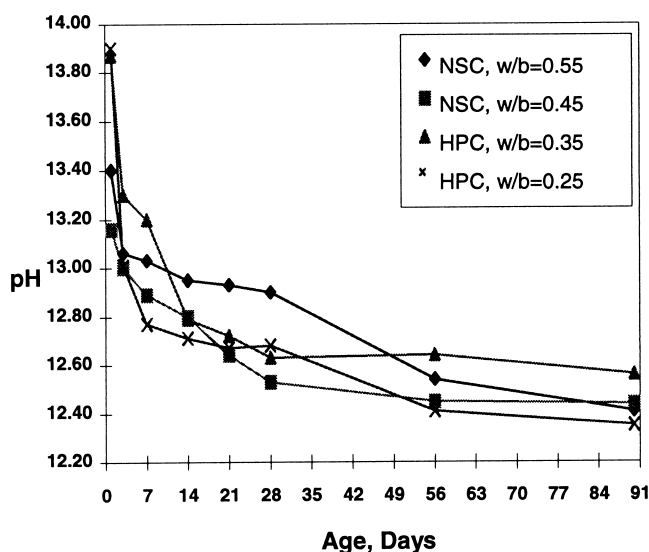


FIG. 9.

Variation of pH of hardened cement paste with age.

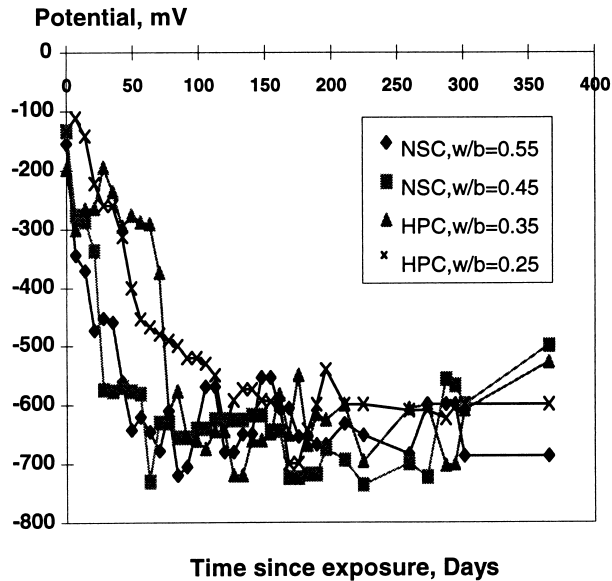


FIG. 10.  
Half-cell potential for ordinary steel bar.

lower initial values. In pastes of NSC mixtures the pH is very stable, ranging only from 13.0 to 12.6 after 90 days. After 90 days, the HSC paste ( $w/b = 0.25$ ) with silica fume shows a decrease in pH to about 12.3, which is still considered sufficient to protect the steel from corroding.

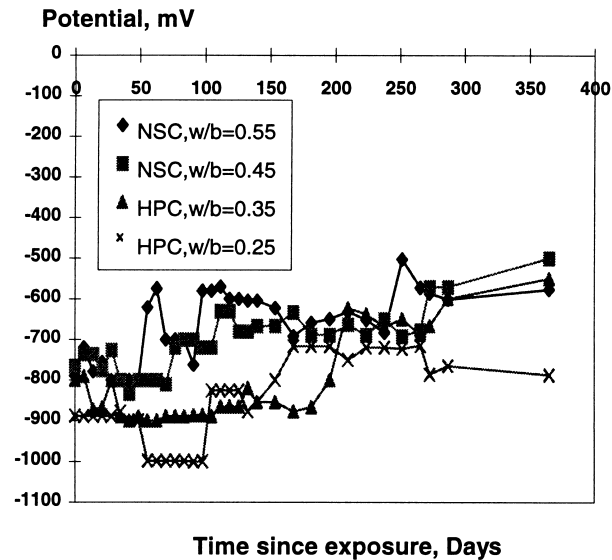


FIG. 11.  
Half-cell potential for galvanized steel bar.

### Corrosion Monitoring by Half-Cell Potential

The half-cell potential readings of specimens subjected to salt water wetting and drying cycles were recorded to compare the performance of the different concrete mixtures and to compare galvanized and ordinary steel reinforcements. The half-cell potential readings, with exposure time of cylindrical specimens with 20 mm cover, are illustrated in Figures 10 and 11. From the potential readings and an assumed threshold value of  $-350$  mV for the ordinary steel bars embedded in both NSC and HSC, it can be seen that the bars corroded after about 3 months time. The bars in NSC mixtures started corroding earlier than those in HSC mixtures. Both HSC and NSC mixtures showed cracking just before and after the half-cell potential values reached the assumed threshold, and there was no obvious difference in the cracking patterns or crack widths. Some specimens with NSC mixtures cracked after an exposure time of only 3 weeks. From the observations, it appears that sufficient cover thickness is necessary in an aggressive environment, even if HSC mixtures are used, for the protection of ordinary reinforcement from corrosion.

Galvanized steel reinforcement showed a different potential behavior. The zinc potential varied from  $-1000$  mV to  $-700$  mV (Fig. 11), and once the zinc coating started to corrode, the half-cell potential values were maintained at  $-600$  mV to  $-500$  mV. In some cases, half-cell potential readings of  $-300$  mV were observed with galvanized steel, and this may be possibly due to non-uniformities in coating thickness for very thin coatings, as shown in Figure 1b. Galvanized steel performance also depends on the thickness of coating, permeability of the concrete, concrete cover and the aggressiveness of the environment. Cracks appeared in some specimens with NSC mixtures after about 2 months of exposure. Crack patterns were observed to be similar to those specimens with ordinary steel reinforcement.

Wolsiefer (12), Omar et al. (13), Al Gahtani et al. (14), Al Saadoun et al. (15), and Ehtesham et al. (2) have used half-cell potential measurements to study the effect of silica fume and blended cements with fly ash on the time required for commencement of corrosion. Wolsiefer (12) tested slabs with 25mm cover made of normal Portland cement concrete and 20% silica fume (by mass of cement) concrete with a w/b of 0.22. The test regimen included immersion in 15% NaCl, (4 days' immersion and 3 days' drying cycles) for 48 weeks. The corrosion of steel was monitored by half-cell potential. The results showed that with blended cement mixtures, the steel reinforcement remained passive and the potential reading remained below  $-100$  mV even after 48 weeks. However, in normal Portland cement concrete mixtures, the potential readings exceeded (numerically) the assumed threshold value ( $-350$  mV) after 7 weeks and showed corrosion of reinforcement as indicated by the corrosion products on the reinforcing steel. Omar et al. (13), Al Gahtani et al. (14), Al Saadoun et al. (15), and Ehtesham (2) also used the same technique. Their results also showed that blended cements delayed substantially the initiation of steel corrosion.

### Conclusions

1. Providing high-performance concrete cover to the reinforcement can increase the time before the commencement of chloride ion-induced corrosion. However, sufficient cover is still necessary in an aggressive environment.

2. The rapid chloride ion penetration test does not have a direct relationship to the rate of corrosion of reinforcement, but is a useful comparative indicator in assessing the relative resistance of different concrete mixtures to chloride ion penetration.
3. Silica fume replacement by 10% (by mass of cement) tends to reduce the pH of the concrete gradually over a long period of time such as 90 days. However, the reduction is still small to affect the rate of corrosion.
4. Galvanized steel can delay the onset of chloride ion-induced corrosion. Use of HPC together with galvanized steel will substantially delay the chloride ion-induced corrosion.

### References

1. F.C. Porter, Corrosion Resistance of Zinc and Zinc Alloys, p. 523, Marcel Dekker Inc., New York, USA, 1994.
2. H. Ehtesham and Rashheduzzaffar, J. Mater. in Civ. Eng. 5, 155 (1993).
3. ASTM: C1202-91, Electrical Indication of Concrete's Ability to Resist Chloride Ion Penetration, 1991.
4. ASTM: C876-91, Standard Test Method for Half-Cell Potentials of Reinforcing Steel in Concrete, 1991.
5. C. Andrade, Cem. Concr. Res. 23, 724 (1993).
6. N. Gowripalan and H.M. Mohamed, Proc. Int. Con. on High-Performance Concrete, and Performance and Quality of Concrete Structures, Florianopolis, Brazil, p. 445, 1996.
7. C. Ozyildirim, Durability of Concrete, Third Int. Con., Nice, France, ACI SP145, p. 503, 1994.
8. S. Misra, A. Yamamoto, T. Tsutsami, and K. Motohashi, Durability of Concrete, Third International Con., Nice, France, ACI SP145, p. 487, 1994.
9. B.A. Suprenant, Concr. Constr. 36, 531 (1991).
10. Ozyildirim, C., ACI Mater. J., 91(2), 197, (1994).
11. O.D. Gjorv, Proc. of the Int. Con. High-Performance Concrete, and Performance and Quality of concrete structures, Florianopolis, Brazil, p. 425, 1996.
12. J.T. Wolsiefer, Durability of Concrete, Second Int. Con., Montreal, Canada, SP126-28, p. 527, 1991.
13. O.S. Baghabra Al Moudi, Rashheduzzafar, M. Maslehuddin, and A.A. Ibrahim Al-Mana, ACI Mater. J. 90, 564 (1993).
14. A.S. Al Gahtani, Rashheduzzafar, and S.S. Al Saadoun, J. Mater. Civ. Eng., 6, 223 (1994).
15. S.S. Al Saadoun, Rashheduzzafar, and A.S. Al Gahtani, J. Mater. Civ. Eng., 5, 356 (1993).